# Action Potential

## JOHN A. WHITE
*Boston University*

I. Basic Properties of the Action Potential

II. Classical Descriptions of the Action Potential

III. Current Topics Related to the Action Potential

## GLOSSARY

**activation** The time-dependent growth of a membrane conductance in response to membrane depolarization.

**all-or-nothing** A term that refers to the property that action potentials, if they occur, have a stereotyped shape that is largely independent of the size and form of the suprathreshold stimulus.

**current clamp** An experimental protocol in which transmembrane current is controlled, usually at a series of constant values, and resulting transmembrane potentials are measured.

**deactivation** The time-dependent reversal of activation in response to membrane hyperpolarization; leads to a decrease in membrane conductance.

**deinactivation** The time-dependent reversal of inactivation, triggered by hyperpolarization; leads to an increase in membrane conductance.

**depolarization** Making membrane potential less negative.

**hyperpolarization** Making membrane potential more negative.

**inactivation** The time-dependent decline of a conductance (e.g., the $Na^+$ conductance), which follows after its activation; triggered by depolarization.

**membrane potential** The voltage difference across the neural membrane, determined by the balance of ionic fluxes across the plasma membrane.

**refractory period** The period immediately after an action potential, in which it is difficult or impossible to induce a second action potential.

**space clamp** The condition in which membrane potential is the same throughout the spatial extent of the cell.

**threshold** The value of membrane current or membrane potential necessary to induce an action potential.

**voltage clamp** An experimental protocol in which membrane potential is controlled, usually in a stepwise fashion, and resulting transmembrane currents are measured.

**voltage-gated ion channels** Transmembrane proteins that open in response to changes in membrane potential, allowing a particular ionic species to cross the membrane.

**The action potential is the all-or-nothing electrical impulse** used to communicate information between neurons and from neurons to muscle fibers. The energy used to generate action potentials is in the form of electrochemical gradients of ions (in particular, sodium and potassium) that are established by ion pumps. The rising phase of action potentials is caused by the autocatalytic activation of many $Na^+$-selective ion channels in response to sufficiently large increases in membrane potential. The falling phase of the action potential is caused by two factors that develop more slowly but dominate the electrical response after a few milliseconds: the inactivation of sodium channels and the activation of potassium channels, both of which occur in response to depolarization. Understanding the diverse mechanisms underlying electrical excitability in neurons remains a rich field of experimental and theoretical study, with wide-ranging implications for human health.

# I. BASIC PROPERTIES OF THE ACTION POTENTIAL

The basic properties of the action potential can be studied using a microelectrode constructed from a glass capillary tube with a fine tip and containing artificial intracellular solution. This microelectrode,

inserted into the cell body or axon of a neuron (Fig. 1a, inset), measures the value of membrane potential relative to the extracellular space. At rest, typical values of membrane potential range from $-40$ to $-90$ mV. Passing positive electrical current into the cell depolarizes it (i.e., makes membrane potential less negative). In response to small depolarizing stimuli, the neuron's response is small as well (Fig. 1a, bottom). In response to larger stimuli, above a threshold value, the response is fundamentally different; the membrane potential quickly rises to a value well above 0 mV and then falls over the course of 1–5 msec to its resting value (Fig. 1a, middle). Often, the falling phase of the action potential undershoots resting potential temporarily. The action potential is said to be all-or-nothing because it occurs only for sufficiently large depolarizing stimuli, and because its form is largely independent of the stimulus for suprathreshold stimuli. In some neurons, a single action potential can be induced by the offset of a hyperpolarizing stimulus
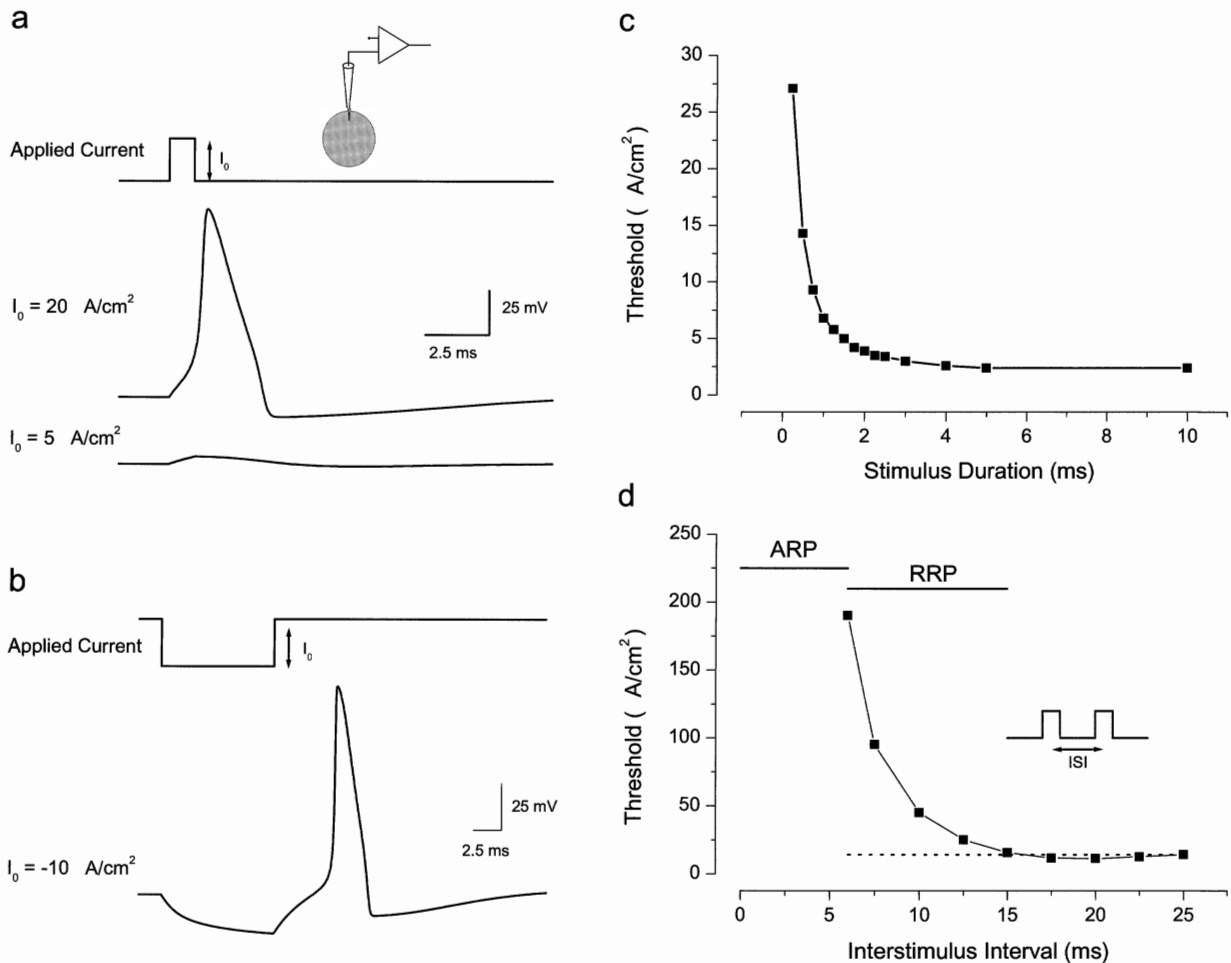


**Figure 1** Basic properties of the action potential. (a) Traces show responses of a simulated space-clamped squid axon ($T = 6.3°C$) to intracellularly injected current pulses of duration 0.5 msec (top trace). The simulated recording configuration is shown in the inset. Sufficiently large inputs evoke all-or-nothing action potentials (middle trace). The response is minimal to subthreshold stimuli (bottom trace). The inset shows the basic recording configuration. (b) A simulation demonstrating anode-break excitation in response to the offset of a hyperpolarizing current pulse (duration = 10 msec). (c) Current threshold (the minimal amplitude of a current step necessary to evoke an action potential) plotted vs stimulus duration. (d) Simulation results demonstrating refractoriness. Two current pulses (duration = 0.5 msec each) were delivered to the model, with interstimulus interval (ISI) varied systematically. The first pulse had magnitude twice the threshold for evoking an action potential. The y-axis shows the magnitude of the second pulse necessary to evoke a spike. For ISI < 15 msec, threshold is above its normal value (dashed line). During the relative refractory period (RRP), threshold is elevated; during the absolute refractory period (ARP), it is not possible to evoke a second action potential.
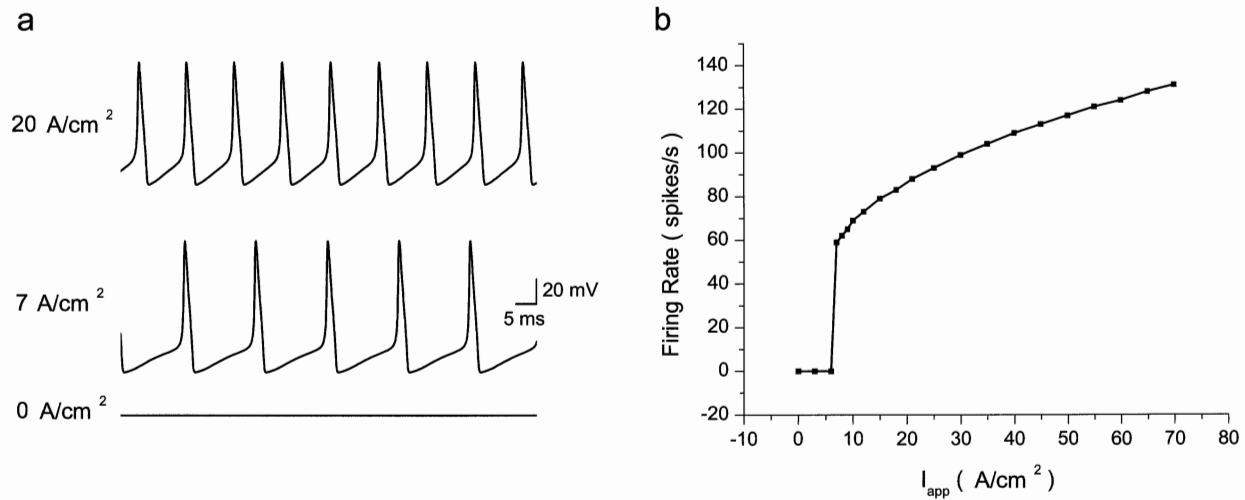
a



20 A/cm$^2$

7 A/cm$^2$

20 mV
5 ms

0 A/cm$^2$

b



Firing Rate ( spikes/s )

$I_{app}$ ( A/cm$^2$ )

**Figure 2** Spike rate depends on the magnitude of applied current. (a) Simulated traces of space-clamped squid giant axon ($T = 6.3°C$) to constant applied current. (b) Firing rate increases with increasing applied current. Note that the minimal firing rate is well above zero spikes/sec.

(Fig. 1b). This phenomenon is called anodal break excitation or rebound spiking.

The value of threshold depends on the duration of the stimulus (Fig. 1c); brief stimuli are required to be larger to evoke an action potential. Threshold also depends on more subtle features of the stimulus, such as its speed of onset. For a short time after an action potential has occurred, it is impossible to evoke a second one (Fig. 1d). This period is referred to as the absolute refractory period (ARP). After the ARP comes the relative refractory period (RRP), in which an action potential can be evoked, but only by a larger stimulus than was required to evoke the first action potential. Stimulation by an ongoing suprathreshold stimulus leads to repetitive firing at a rate that is constant once any transients have settled out (Fig. 2a). The rate of repetitive firing increases with increasing depolarization (Fig. 2b), eventually approaching the limit imposed by the ARP.

Once initiated, the action potential propagates down the axon at an approximately constant velocity. The leading edge of the action potential depolarizes adjacent unexcited portions of the axon, eventually bringing them to threshold. In the wake of the action potential, the membrane is refractory, preventing reexcitation of previously active portions of the cell. In unmyelinated axons, the action potential travels smoothly, with constant shape and at constant velocity. In myelinated axons, conduction is saltatory: The action potential "jumps" nearly instantaneously from one node of Ranvier to the next, greatly increasing the speed of propagation.

## II. CLASSICAL DESCRIPTIONS OF THE ACTION POTENTIAL

### A. Electrochemical Potentials and Voltage-Dependent Membrane Conductances

Changes in electrical potential in excitable cells are driven by movement of ions through ion-specific membrane conductances. For a perfectly specific conductance $G$, the current across the membrane $I = G \times (V_m - V_n)$, where $V_m$ is the electrical potential across the membrane and $V_n$ is the equilibrium potential for the ion, given by the Nernst equation:

$$V_n = \frac{RT}{z_n F} \ln \left( \frac{[X_n]^o}{[X_n]^i} \right)$$

where $R = 8.314$ J/(mol K) is the gas constant, $T$ is absolute temperature, $z_n$ is the valence of ion $n$, $F = 9.648 \times 10^4$ C/mol and is Faraday's constant, $[X_n]^o$ is the outer concentration of ion $n$, and $[X_n]^i$ is the inner concentration of ion $n$. Intuitively, the equilibrium potential is the value of membrane potential at which ionic fluxes due to concentration gradients and voltage gradients cancel one another, leading to zero net flux of the ion. Note that ionic

current, as defined, is positive for outward flux of a positive ion. For neurons, $[Na^+]^o > [Na^+]^i$; consequently, $V_{Na}$ typically ranges from 40 to 50 mV and $I_{Na} < 0$. In contrast, $[K^+]^i > [K^+]^o$; $V_K$ ranges from $-70$ to $-100$ mV and $I_K > 0$. The fact that resting membrane potential is far from $V_{Na}$ and close but typically not equal to $V_K$ implies that these ions are out of equilibrium, and thus that there is a constant trickle of each, even at rest. This flux is opposed by energy-expending ionic pumps, most notably the $Na^+/K^+$ ATPase, which serve to maintain $Na^+$ and $K^+$ concentration gradients and, consequently, equilibrium potentials.

Among the first quantitative clues regarding the mechanisms underlying the action potential came from ionic substitution experiments demonstrating that $Na^+$ and $K^+$ are the primary ions responsible for the phenomenon. Other early experiments demonstrated that membrane conductance, but not membrane capacitance, changes during the course of the action potential. Together, these results suggested the hypothesis that fluxes of $Na^+$ and $K^+$, driven by changes in ion-specific conductances, are responsible for the action potential. It is important to note that changes in membrane potential are not induced by changes in intracellular concentrations of $Na^+$ and $K^+$: Ionic fluxes during individual action potentials are small enough that concentrations remain essentially unperturbed. Instead, ionic fluxes alter $V_m$ by changing the distribution of charge very near the membrane.

## B. The Hodgkin–Huxley Model of the Space-Clamped Action Potential

Researchers in the middle of the 20th century hypothesized that the $Na^+$ and $K^+$ conductances underlying the action potential are "gated" (i.e., turned on and off) by changes in membrane potential. To test this hypothesis, they devised methods to measure ionic fluxes while controlling membrane potential $V_m$ at a fixed value throughout the length of the axon. The process of controlling $V_m$, called voltage clamping, simplifies the behavior of the hypothesized voltage-dependent "gates." The process of making $V_m$ the same throughout the axon, called space clamping, prevents complex spatial spread of excitation. Under these conditions, $Na^+$ and $K^+$ fluxes can be isolated either by manipulation of ionic concentrations (and thus equilibrium potentials) or by using specific blockers of particular conductances. (Tetrodotoxin is the classic blocker of $Na^+$ conductances; tetraethyl ammonium blocks many $K^+$ conductances.) Isolated $Na^+$ and $K^+$ fluxes from simulations are shown in Fig. 3 for many values of membrane potential. As hypothesized, these fluxes are voltage dependent. $Na^+$ and
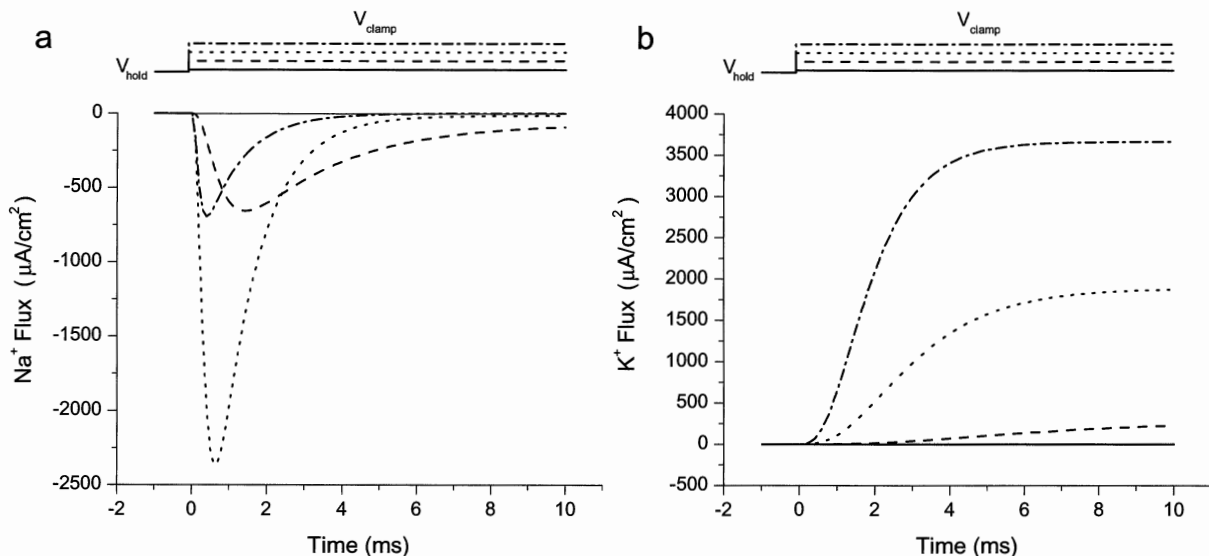


**Figure 3**  Simulated responses to voltage-clamp stimuli. Simulated $Na^+$ (a) and $K^+$ (b) in response to voltage-clamp steps from a holding potential of $-90$ mV to clamp potentials of $-80$ (solid lines), $-40$ (dashed lines), 0 (dotted llines), and 40 mV (dashed and dotted lines). The $Na^+$ flux is inward (negative) and is characterized by rapid activation and slower inactivation. The $K^+$ flux is outward (positive) and activates significantly more slowly than the $Na^+$ flux.

$K^+$ fluxes differ in several important aspects. First, they are opposite in sign for most values of membrane potential: The $Na^+$ flux depolarizes the neuron, whereas the $K^+$ flux hyperpolarizes the cell. Second, the $Na^+$ flux turns on ("activates") much more quickly than the $K^+$ flux. Third, the $Na^+$ flux turns off ("inactivates") after a brief period of depolarization. In contrast, the $K^+$ conductance remains activated in response to a prolonged depolarizing stimulus.

A watershed event in the history of neuroscience was the development by Hodgkin and Huxley of a relatively simple mathematical model, derived from voltage-clamp studies of the giant axon of the squid, that accounts for the generation and propagation of the action potential. The Hodgkin–Huxley model describes the membrane as an electrical circuit (Fig.

4a) that includes descriptions of membrane capacitance $C_m$; voltage-gated, $Na^+$- and $K^+$-selective conductances ($G_{Na}$ and $G_K$, respectively), each in series with a battery representing the appropriate equilibrium potential; and a constant "leak" conductance that passes more than one ion. Mathematically, the Hodgkin–Huxley model includes four differential equations, which describe how the derivatives of membrane potential and three "gating variables" (variables that range between 0 and 1 and determine the values of voltage-gated conductances) behave. Two time- and voltage-dependent gating variables determine the size of the $Na^+$ conductance: The $m$ gate captures the rapid activation of the $Na^+$ conductance after a step depolarization, whereas the $h$ gate describes the slower inactivation process by which the
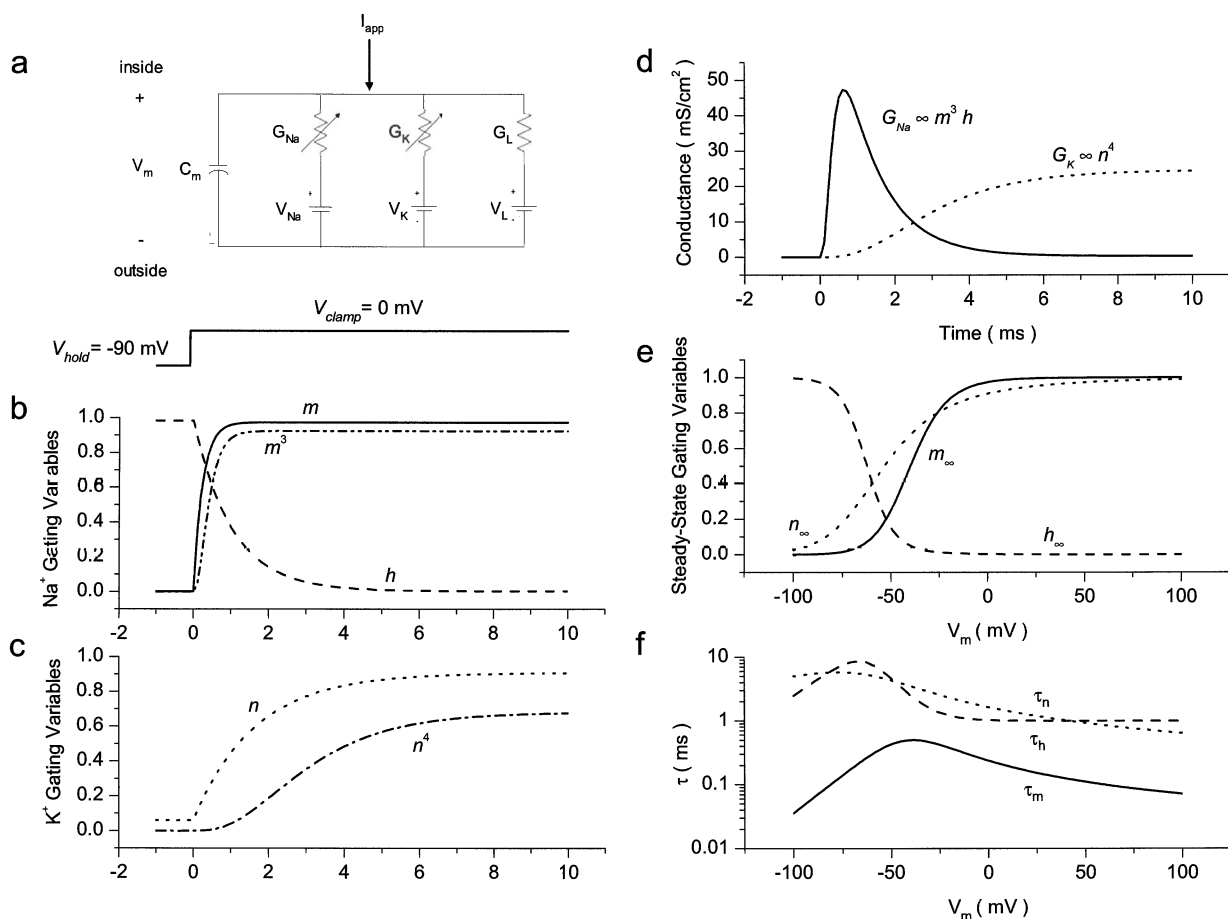
**Figure 4** The Hodgkin–Huxley model of voltage-gated $Na^+$ and $K^+$ conductances. (a) Electrical circuit representation of the Hodgkin–Huxley model of squid giant axon under space-clamped conditions. (b–d) Responses of the Hodgkin–Huxley gating variables to a voltage-clamp step from $V_{hold} = -90$ mV to $V_{clamp} = 0$ mV. The $m$ and $h$ gates determine the value of $G_{Na} \propto m^3 h$. The $n$ gate determines the value of $G_K \propto n^4$. (e) Steady-state values of $m$, $h$, and $n$ for the entire physiologically relevant range of membrane potential $V_m$. (f)Time constants describing how quickly the gating variables $m$, $h$, and $n$ reach their steady-state values, plotted vs $V_m$. Note the log scale on the $y$-axis.

### Table I
#### Definitions and Units of Mathematical Symbols

| | |
|---|---|
| $C_m$ | Membrane capacitance per unit area ($\mu F/cm^2$) |
| $\bar{G}_{Na}, \bar{G}_K$ | Maximal values of voltage-gated $Na^+$ and $K^+$ conductances per unit area ($mS/cm^2$) |
| $G_{Na}, G_K$ | Voltage-gated $Na^+$ and $K^+$ conductances per unit area ($mS/cm^2$) |
| $G_L$ | Leak conductance per unit area ($mS/cm^2$) |
| $m, h, n$ | Voltage-dependent gating variables that determine magnitudes of voltage-gated conductances (dimensionless) |
| $m_\infty, h_\infty, n_\infty$ | Voltage-dependent steady-state values of gating variables (dimensionless) |
| $\tau_m, \tau_h, \tau_n$ | Voltage-dependent time constants associated with gating variables (msec) |
| $\frac{dm}{dt}, \frac{dh}{dt}, \frac{dn}{dt}$ | Time derivatives of gating variables (1/msec) |
| $V_{Na}, V_K$ | Equilibrium potentials for $Na^+$ and $K^+$ (mV) |
| $V_L$ | Reversal potential for the multi-ion leak conductance (mV) |
| $I_{app}$ | Applied current flux ($\mu A/cm^2$) |
| $V_m$ | Membrane potential (mV) |
| $\frac{dV_m}{dt}, \dot{V}_m(t)$ | Time derivative of membrane potential (mV/msec) |

$Na^+$ conductance turns off in response to prolonged depolarization. One gating variable, the $n$ gate, describes voltage-dependent activation of the $K^+$ conductance $G_K$. An additional conductance (the leak conductance $G_L$) is voltage independent and small. In mathematical terms, the Hodgkin–Huxley equation is written as follows, with symbols defined in Table I:

$$C_m \frac{dV_m}{dt} = -[G_{Na}(V_m - V_{Na})$$

$$+ G_K(V_m - V_K) + G_L(V_m - V_L)] + I_{app}$$

$$G_{Na} = \bar{G}_{Na} m^3 h \qquad G_K = \bar{G}_K n^4$$

$$\frac{dm}{dt} = \frac{m_\infty(V_m) - m}{\tau_m(V_m)} \qquad \frac{dh}{dt} = \frac{h_\infty(V_m) - h}{\tau_h(V_m)}$$

$$\frac{dn}{dt} = \frac{n_\infty(V_m) - n}{\tau_n(V_m)}$$

In response to a step change from an initial value of membrane potential (often referred to as the holding potential, $V_{hold}$) to the clamp potential, $V_{clamp}$, each of the Hodgkin–Huxley gating variables ($m$, $h$, and $n$) changes from an initial value to a steady-state value with an exponential time course (Figs. 4b and 4c). The steady-state values ($m_\infty, h_\infty$, and $n_\infty$) and exponential time constants ($\tau_m, \tau_h$, and $\tau_n$) are determined solely by the current value of $V_m$, which equals $V_{clamp}$ for voltage-clamp experiments (Figs. 4e and 4f). The initial values of the gating variables are determined by the holding potential. $G_{Na}$ is proportional to $m^3 \times h$; $G_K$ is proportional to $n^4$ (Figs. 4b–4d). The powers to which the gating variables $m$ and $n$ are raised were used by Hodgkin and Huxley to induce small delays in activation of the conductance in order to better match experimental data.

## C. The Hodgkin–Huxley Model Accounts for the Basic Properties of the Action Potential

Although the Hodgkin–Huxley model is incorrect in some details (see Section III.A), it can account for many of the basic properties of the neuronal action potential. For example, two properties of the $m$ gate account for the phenomenon of the all-or-nothing action potential with a distinct threshold in response to a particular type of stimulus:

1. Because the $m$ gate activates (opens) with depolarization, and its activation leads to further depolarization, this gate is prone to autocatalytic "positive feedback" that can magnify a small depolarization into a full-blown action potential. The current threshold for firing an action potential is the amount of current required to engage this cycle of positive feedback (see Section III.D for a discussion of the threshold value of membrane potential). In contrast with the $m$ gate, the $h$ and $n$ gates react to oppose depolarization ($h$ because it becomes smaller with depolarization, and $n$ because its activation increases the size of an outward $K^+$ current).

2. The $m$ gate is much faster than the $h$ and $n$ gates (Fig. 4e). The speed of the $m$ gate means that the rapid rising phase of the action potential can occur before the stabilizing influences of the $h$ and $n$ gates can engage to bring $V_m$ back to near resting potential. The speed of inactivation of $h$ (i.e., its decrease with depolarization) and activation of $n$ determine the width of the action potential.

Traces of each of the gating variables during the course of a depolarization-induced action potential are shown in Fig. 5a. Like spike threshold and spike duration, the phenomena of absolute and relative refractory periods can be accounted for by tracking gating variables. The ARP is associated with elevated values of $n$ and, most important, greatly reduced

values of $h$ after a spike (Fig. 5a). These factors make it impossible for a second spike to be elicited soon after the first. The RRP lasts as long as it takes for the $h$ and $n$ gates to return to their baseline values (about 15 msec in squid giant axon).

At resting potential, the voltage-gated $Na^+$ conductance is partially inactivated in that the $h$ gate is partly closed and the $n$ gate is partly open (Figs. 4 and 5). Hyperpolarizing the neuron below resting potential increases the value of $h$, in a process called deinactivation, and decreases the value of $n$, in a process called deactivation. Deinactivation of the $Na^+$ conductance and deactivation of the $K^+$ conductance can leave the neuron more excitable after hyperpolarization, and thus can account for anodal break excitation (Fig. 5b), also known as rebound spiking. Neurons typically fire only one rebound spike because after that spike the $Na^+$ and $K^+$ conductances return to their baseline states and the cell returnes to its resting level of excitability.

The first major success of the Hodgkin–Huxley model was that this relatively simple model, derived from voltage-clamp experiments, accounted successfully for many aspects of the action potential in the current-clamped and space-clamped axon. Even more impressive, and strikingly demonstrative of the level of understanding this model represents, was its ability to accurately account for the shape and velocity of the propagating action potential. The quantitative arguments involved are complex and will not be discussed here, but Fig. 6 shows qualitatively how action potentials propagate in unmyelinated axons.
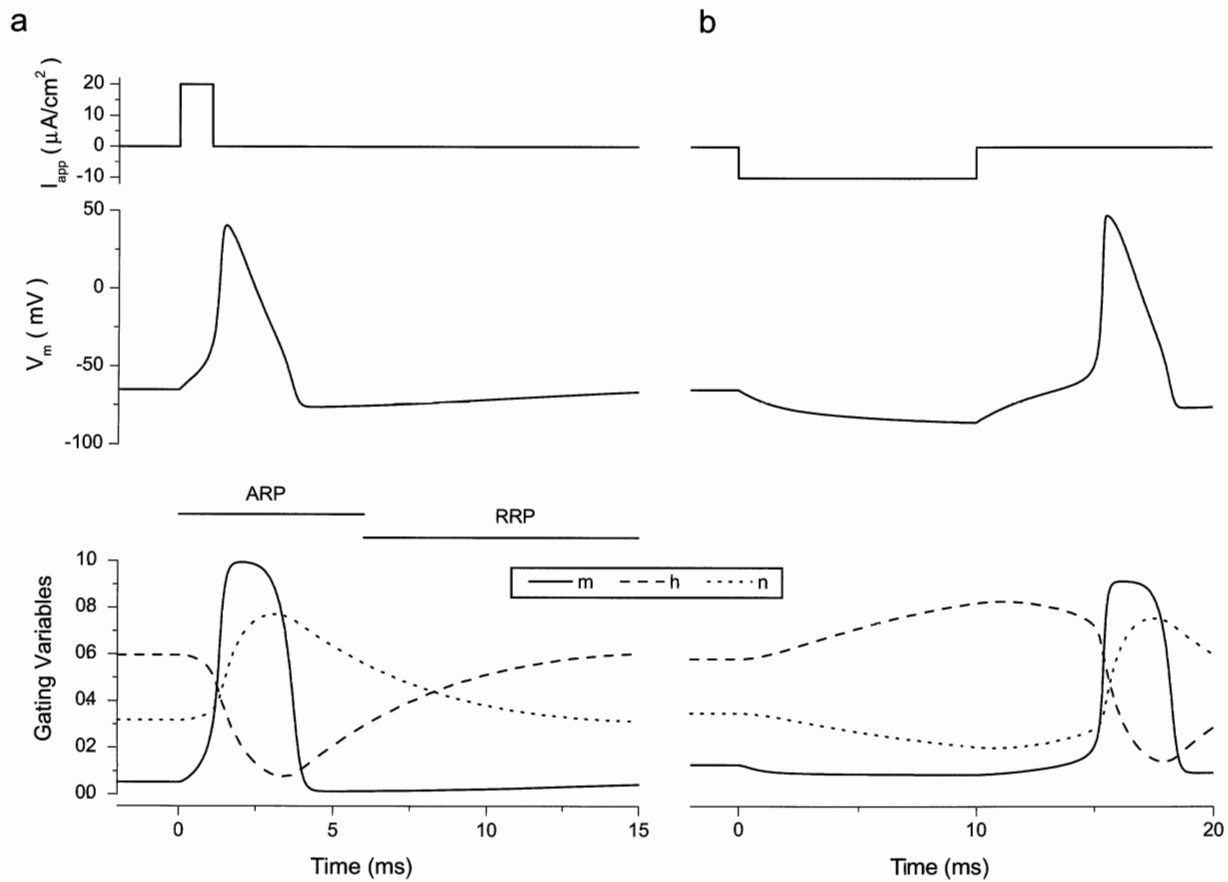


**Figure 5** The Hodgkin–Huxley model accounts for axonal excitability. (a) From top to bottom, applied current $I_{app}$, membrane potential $V_m$, and each of the gating variables are plotted vs time. Curves were derived from the Hodgkin–Huxley model at 6°C. The rapid activation of the $m$ gate underlies the action potential in response to this brief current pulse. The slower inactivation of the $h$ gate and activation of the $n$ gate repolarize the membrane a few milliseconds later. The duration of the absolute and relative refractory periods (ARP and RRP, respectively) is controlled by the duration of $h$ gate inactivation and $n$ gate activation. (b) After a hyperpolarizing input, the Hodgkin–Huxley model (6°C, with enhanced density of the $Na^+$ conductance) can produce a rebound spike (also known as anode break excitation). Data are plotted in the same order as in (a). Deactivation of the $n$ gate and deinactivation of the $h$ gate underlie this phenomenon.

Direction of Propagation

Refractory Membrane    Spiking Membrane

Charging Membrane
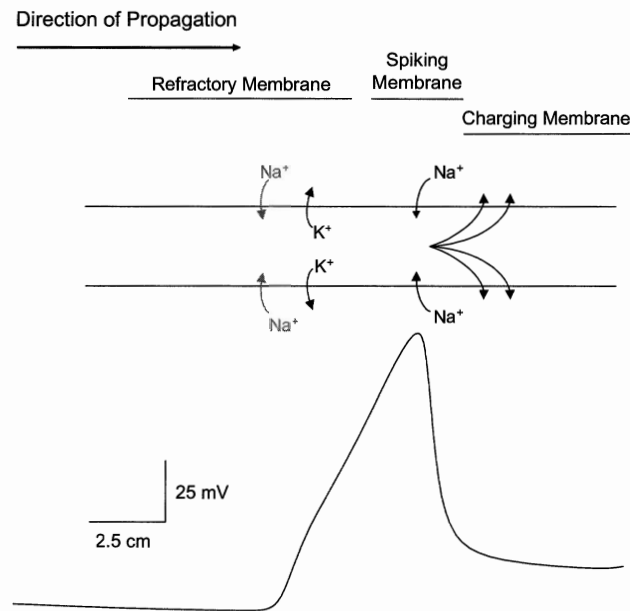
Na⁺    Na⁺

K⁺

K⁺

Na⁺    Na⁺

25 mV

2.5 cm

**Figure 6**   Propagation of the action potential in an unmyelinated axon. (Top) Schematic of the unmyelinated axon showing the sequence of events as an action potential propagates from left to right. The point of maximal Na$^+$ flux characterizes the locus where $V_m$ is greatest. Positive charge from this point spreads to the right, gradually depolarizing the membrane on the leading edge of the action potential until threshold is reached. At the trailing edge of the action potential, to the left, the membrane is refractory. (Bottom) "Snapshot" of $V_m$ plotted vs axial distance for the propagating action potential, with an assumed conduction velocity of 20 m/sec. Note that the form of the action potential is reversed when plotted vs distance rather than time.

Membrane potential reaches its peak value near the position of maximal Na$^+$ flux. Adjacent, unexcited membrane (Fig. 6, right) is depolarized by positive current from the site of Na$^+$ flux. Eventually, this depolarization is large enough that the membrane at the leading edge is excited as well. The membrane in the wake of the action potential is refractory (i.e., dominated by small $G_{Na}$ and large $G_K$, and thus unable to spike) and thus unlikely to be reexcited. Elaborations of this model can account for saltatory conduction in myelinated axons.

## III.  CURRENT TOPICS RELATED TO THE ACTION POTENTIAL

### A.  Voltage-Gated Ion Channels Underlie Voltage-Dependent Membrane Conductances

In the past two decades, improvements in recording methodologies, pioneered by the group of Sakmann and Neher, as well as an explosion of knowledge in the field of molecular biology have demonstrated directly that membrane protein assemblies called ion channels underlie voltage-gated conductances in neurons and

other excitable cells. The main ($\alpha$) subunit of voltage-gated Na$^+$ channels (Fig. 7a) is a membrane protein approximately 2000 amino acids in length and has a molecular weight $> 200,000$. This protein includes four domains, each of which consists of six putative transmembrane segments. A smaller $\beta$ subunit is not necessary to form the channel but is crucial for regulating aspects of channel function such as the speed of inactivation. The main subunit of the K$^+$ channel has a very similar structure, except that the each protein codes for only one domain. Thus, four $\alpha$ subunits are necessary to form a K$^+$ channel.

Recordings from single channels (Fig. 7b) typically reveal two conductance states: "open" and "closed." Switching between open and closed states appears random, but the probability that the channel is in the open state varies with membrane potential. These probabilities correspond approximately to the values of gating variables in the Hodgkin–Huxley formulation. Sums of repeated recordings from an individual ion channel show behavior that is very similar to the macroscopic behavior of the channel population (Fig. 7b). Sophisticated analyses of single-channel recordings yield probabilistic models that can account for both microscopic and macroscopic behavior. These
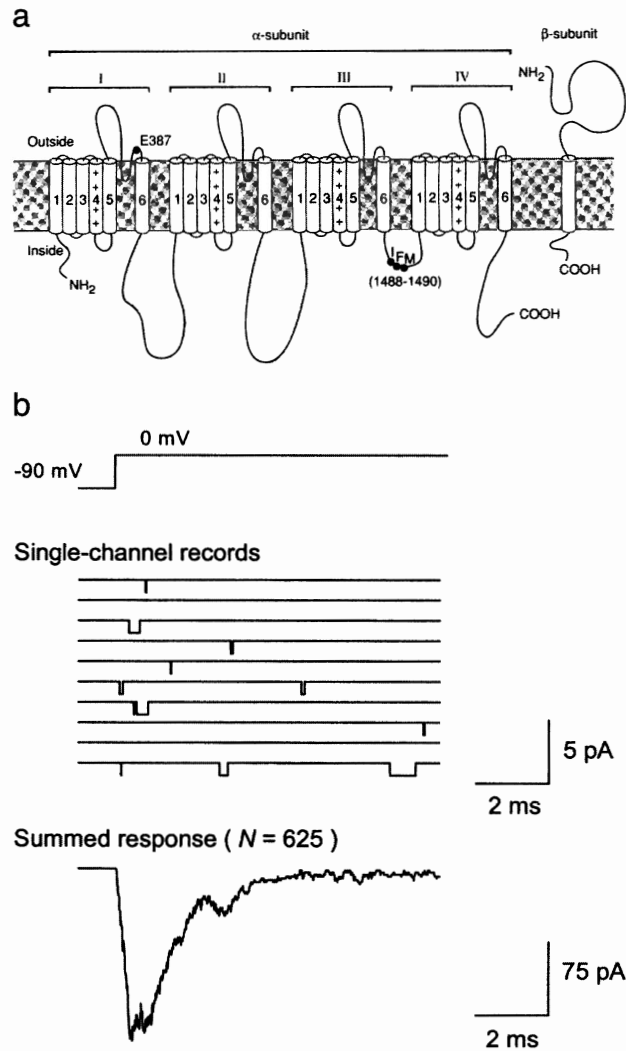
**Figure 7**  Na$^+$ channels underlie the voltage-gated Na$^+$ conductance. (a) Putative structure of the $\alpha$ and $\beta$ subunits of the rat brain Na$^+$ channel (IIA). Roman numerals indicate the domains of the $\alpha$ subunit, each of which includes six putative transmembrane segments. Indicated residues are implicated in binding the channel blocker tetrodotoxin (E387) and in forming the inactivation gate (IFM 1488–1490) (adapted from Ashcroft (2000)). (b) The 10 middle traces show simulated single-channel recordings from a Na$^+$ channel under voltage clamp. The top trace shows the voltage-clamp command. The bottom trace shows the sum of 625 single-channel records.

models are similar in structure to Hodgkin–Huxley-type models but different in some details. For example, careful analysis of recordings from single Na$^+$ channels shows that their inactivation state is not controlled by an activation-independent process like the $h$ gate but, rather, that Na$^+$ channels must activate before they can inactivate.

Experiments with channels that have been subjected to site-directed mutations have revealed close connections between particular loci on the protein and specific aspects of channel behavior. Among the properties that have been tied to specific loci on the $\alpha$ subunit are those of pore formation, ionic selectivity, voltage dependence, inactivation, and blockage by specific toxins (Fig. 7a).

## B. Diversity of Mechanisms Contributing to Neuronal Excitability

In the approximately 50 years since the development of the Hodgkin–Huxley model, researchers have discovered many ion channel-based mechanisms for generating and controlling electrical activity in neurons. Often, these mechanisms rely on Na$^+$, Ca$^{2+}$, and K$^+$ channels. Sodium channels are relatively consistent in

their properties from case to case but do show some variety. In particular, some $Na^+$ channels do not exhibit fast inactivation; it is not clear whether these noninactivating $Na^+$ channels are a separate population from the typical, fast-inactivating $Na^+$ channels or a subset of the fast-inactivating $Na^+$ channels that have slipped into a different "mode" of gating. Calcium and potassium channels show more diversity than $Na^+$ channels. In particular, different classes of $Ca^{2+}$ and $K^+$ channels show widely diverse properties with regard to the presence and speed of inactivation, pharmacological properties, and voltage ranges of activation. Some $K^+$ channels are sensitive to both membrane potential and the local intracellular concentration of $Ca^{2+}$, giving rise to interesting interactions between these two systems.

## C. Modulation of Voltage-Gated Ion Channels

The properties of voltage-gated ion channels are not static. Many neuromodulators have been shown to alter ion channel function and the properties of action potentials by phosphorylating or dephosphorylating one or more sites on the channel protein. A host of neuronal firing properties, including spike width, average firing rate, and refractory period, are subject to metabolic control.

Ion channel expression profiles and neuromodulatory states can have profound consequences for neuronal function. A striking example of this point derives from thalamic relay neurons (Fig. 8). Depending on the level of depolarization or neuromodulatory state, these cells have two distinct firing modes. When relay neurons are hyperpolarized, they exhibit rhythmic bursting (Fig. 8a). The long interburst interval is determined by interaction of the low-threshold $Ca^{2+}$ current and slowly activating, inwardly rectifying cation current. Superimposed on each slow $Ca^{2+}$ spike are many fast action potentials, mediated by $Na^+$ and $K^+$ channels. When relay neurons are depolarized, either by electrical current or any of a number of neuromodulators, the low-threshold $Ca^{2+}$ channels and inwardly rectifying cation channels are unimportant and the neurons fire in a tonic pattern much more reminiscent of the Hodgkin–Huxley model (Fig. 8b).

## D. Mathematical Analyses of Neuronal Excitability

Although much about neuronal excitability can be learned by simply tracking changes in gating variables of the Hodgkin–Huxley-style model, computational neuroscientists and applied mathematicians have used mathematically based techniques to gain more general (and thus deeper) insights. Mathematical approaches
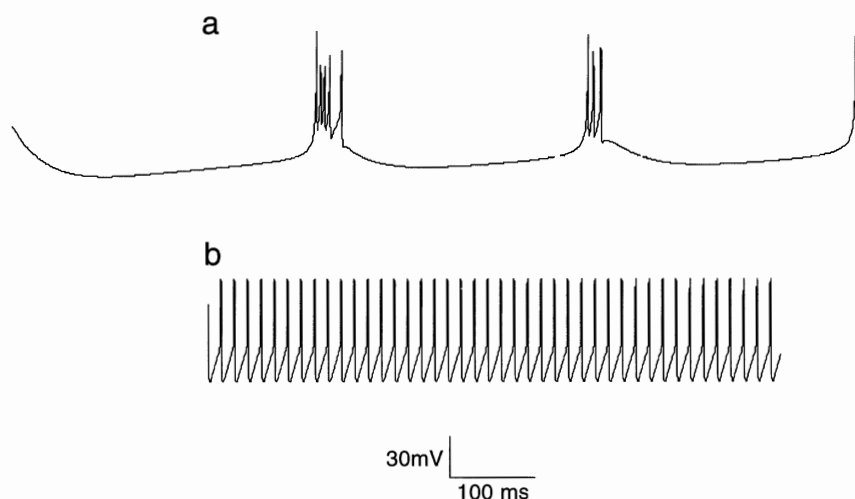
**Figure 8** Thalamic relay neurons show two distinct firing modes. Shown are simulated responses of a thalamic relay neuron [Figure generated using the computational model from D. A. McCormick and J. R. Huguenard (1992). A model of the electrophysiological properties of thalamocortical relay neurons. *J. Neurophysiol.* **68**, 1384–1400]. (a) Under hyperpolarized conditions, relay neurons fire in an oscillatory manner. Slow oscillations are generated by interactions of the transient $Ca^{2+}$ current $I_t$ and the slow, hyperpolarization-activated cation current $I_h$. Fast action potentials, mediated by $Na^+$ and $K^+$, occur at the peaks of the $Ca^{2+}$ spikes. (b) Depolarization by any of a number of means (e.g., current injection or neuromodulation) puts the neuron in a "tonic firing" mode. In this mode, $I_t$ is inactivated and $I_h$ is deactivated. Consequently, the cell's behavior is dominated by the $Na^+$ and $K^+$ currents exclusively.

based on the techniques of nonlinear dynamics have been successful in identifying the particular features that determine a host of important features of neuronal excitability, including threshold, the relationship between sustained firing rates and applied current, and particular patterns of bursting.

Figure 9 shows how nonlinear dynamics can be applied to understand neuronal threshold. Figures 9a and 9b show results from simulations of the Hodgkin–Huxley equations with zero applied current but two different initial conditions in membrane potential. As Figs. 9a and 9b demonstrate, excitable cells can be exquisitely sensitive to initial conditions. Examining the time derivative of membrane potential $\dot{V}_m(t)$ shortly after the perturbation in initial conditions gives insight into this phenomenon. Figure 9c shows results from hundreds of simulations conducted over a large range of initial values $V_0$. $\dot{V}_m(t)$, evaluated at $t = 0.5$ msec, is plotted vs $V_0$ (solid line; the value $t = 0.5$ msec was chosen because this is long enough for the $m$ gate to react significantly to the perturbation away from resting potential but short enough that the $h$ or $n$ gates remain relatively near their resting values). Also plotted

are the contributions to $\dot{V}_m(0.5)$ from $Na^+$ conductance (dashed line) as well as $K^+$ and leak conductances (dotted line). These contributions can be obtained easily from the Hodgkin–Huxley equation describing $\dot{V}_m(t)$. The effect of the $Na^+$ conductance is to elevate $\dot{V}_m(t)$; the effect of the $K^+$ conductance is to reduce $\dot{V}_m(t)$.

Figure 9d shows a magnified view of $\dot{V}_m(0.5)$ in the region near spike threshold. The plot shows two zero-crossings, at $V_0 = -65$ and $-59$ mV. These zero crossings, often called fixed points, are especially important because where $\dot{V}_m(t) = 0$, membrane potential $V_m$ is by definition not changing, meaning that $\dot{V}_m$ has the potential to remain fixed at that point indefinitely (for a system with constant parameters). The slope of the curve at each zero crossing tells us much about the stability of that fixed point in response to small fluctuations (e.g., due to noise). For example, consider the special case of no perturbation. In this case, $V_0$ equals resting potential ($-65$ mV), which we expect to be a fixed point. For $V_m$ slightly less than $-65$ mV, $\dot{V}_m(0.5) > 0$, implying that $V_m$ will return to its resting value. For $V_m$ slightly higher than $65$ mV, $\dot{V}_m(0.5) < 0$, implying again that $V_m$ will return to
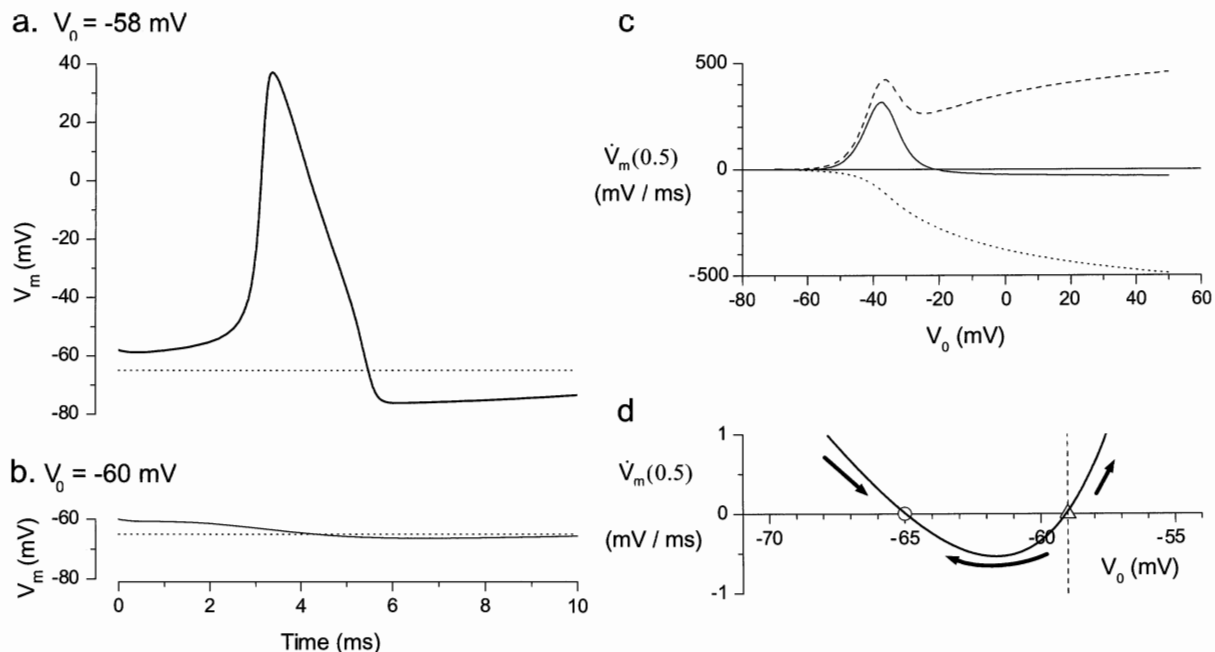


**Figure 9**  Threshold of the Hodgkin–Huxley model can be explained by examining the stability of "fixed points." (a, b) Spiking behavior in the Hodgkin–Huxley model is very sensitive to $V_0$, the initial value of voltage. Resting potential ($-65$ mV) is depicted by the dotted lines. (c) $\dot{V}(0.5)$, the time derivative of membrane potential at $t = 0.5$ msec, plotted vs $V_0$. Also plotted are the contributions of $G_{Na}$ (dashed line), as well as $G_K$ and $G_L$ (dotted line), to $\dot{V}(0.5)$. The contribution of $G_L$ is minimal because this conductance is very small. (d) A magnified plot of $\dot{V}(0.5)$ vs $V_0$. Two fixed points [points where $\dot{V}(0.5) = 0$] are shown. As indicated by the arrows, the sign of $\dot{V}(0.5)$ makes the solution flow toward the open circle at $(-65, 0)$, indicating stability; the solution flows away from the open triangle at $(-59, 0)$, indicating instability. For $V_0 > -59$ mV, an action potential will be generated.

−65 mV. The value $V_m = -65$ mV is said to be a stable fixed point because after small perturbations above or below that value, $V_m$ will return to it.

Next, consider the fixed point at $V_0 = -59$ mV. In this case, $\dot{V}_m(0.5) < 0$ for $V_m < V_0$, and $\dot{V}_m(0.5) > 0$ for $V_m > V_0$. This result implies that this fixed point is unstable: After small perturbations above or below $V_0$, $V_m$ will move away from the fixed point. The implication of this fact is that the point $V_0 = -59$ mV serves as a threshold. For $V_0 < -59$ mV, the model returns to resting potential (Fig. 9a); for $V_0 > -59$ mV, $V_m$ rapidly increases as the action potential begins [Fig. 9b; in these cases, $\dot{V}_m(t)$ continues to evolve, eventually bringing the cell to rest]. For these simulations, the fixed point at $V_0 = -59$ mV corresponds exactly with the threshold for generation of an action potential (vertical dashed line in Fig. 9d).

## E. Backpropagation of the Action Potential

In the traditional view, information flow in the mammalian neuron is in one direction only: The dendrite receives input from the presynaptic population, the soma integrates this information, the decision regarding whether or not to fire an action potential is made at or near the axon hillock, and the action potential is propagated to other neurons by the axon. This view has been amended in recent years as scientists have developed techniques for recording simultaneously from multiple locations within the neuron (e.g., the soma and a primary dendrite). In pyramidal neurons of layer V of neocortex, for example, suprathreshold synaptic input to the apical dendrites leads to initiation of an action potential near the soma. This action potential can then travel back from the soma toward the distal end of the apical dendrite. The reliability of backpropagation depends on recent patterns of input and spike generation. Given the crucial role of dendritic depolarization for synaptic plasticity, backpropagating action potentials may be important for experience-dependent alterations of neuronal circuitry in learning and memory.

## F. Diseases Related to Mutations in Ion Channels

Given the central role that electrical excitability plays in nervous system function, it is not surprising that mutations of voltage-gated ion channels alter neuronal function. Although work in this area is just beginning, a host of maladies have been associated with nonlethal mutations of neuronal voltage-gated channels, including the following:

- Generalized epilepsy with febrile seizures, so-named because patients have fever-induced seizures that develop later in life into seizures without a clear trigger, is associated in some cases with a rare mutation of the $\beta_1$ subunit of the $Na^+$ channel. This mutation may promote epilepsy by slowing the inactivation process in neuronal $Na^+$ channels, leaving the brain hyperexcitable.

- Benign familial neonatal epilepsy is associated with mutations that lead to reduced expression of slow, voltage-gated $K^+$ channels of the KCNQ family, thereby leaving some neurons hyperexcitable.

- Some forms of episodic ataxia, a condition of triggered events of imbalance and uncoordinated movements, has been associated with many missense mutations of the $K_v1.1$ channel, which gives rise to an inactivating $K^+$ conductance. Ataxia-associated mutations of $K_v1.1$ have been shown to lead to pathologically rapid deactivation, enhanced inactivation, and increases in the threshold of activation. These disparate changes all have the effect of broadening the neuronal action potential, but it is not known how the broadened spike may lead to ataxia.

### See Also the Following Articles

ELECTRICAL POTENTIALS • ELECTRO-ENCEPHALOGRAPHY (EEG) • EVENT-RELATED ELECTROMAGNETIC RESPONSES • ION CHANNELS • NEURON • NEURAL NETWORKS

### Suggested Reading

Aidley, D. J., and Stanfield, P. R. (1996). *Ion Channels: Molecules in Action*. Cambridge Univ. Press, Cambridge, UK.

Ashcroft, F. M. (2000). *Ion Channels and Disease*. Academic Press, San Diego.

Häusser, M., Spruston, N., and Stuart, G. (2000). Diversity and dynamics of dendritic signaling. *Science* **290,** 739–744.

Hille, B. (2001). *Ionic Channels of Excitable Membranes*, 3rd ed. Sinauer, Sunderland, MA.

Johnston, D., and Wu, S. M.-S. (1995). *Foundations of Cellular Neurophysiology*. MIT Press, Cambridge, MA.

Koch, C. (1999). *Biophysics of Computation*. Oxford Univ. Press, New York.

Koch, C., and Segev, I. (Eds.) (1998). *Methods in Neuronal Modeling*, 2nd ed. MIT Press, Cambridge, MA.

Nicholls, J. G., Martin, A. R., Wallace, B. G., and Fuchs, P. A. (2000). *From Neuron to Brain*, 4th ed. Sinauer, Sunderland, MA.

Sakmann, B., and Neher, E. (Eds.) (1995). *Single-Channel Recording*, 2nd ed. Plenum, New York.

Weiss, T. F. (1996). *Cellular Biophysics*. MIT Press, Cambridge, MA.

White, J. A., Rubinstein, J. T., and Kay, A. R. (2000). Channel noise in neurons. *Trends Neurosci.* **23,** 131–137.